



Published in final edited form as:

Nature. ; 480(7378): 557–560. doi:10.1038/nature10656.

GlcNAcylation of a histone methyltransferase in retinoic-acid-induced granulopoiesis

Ryoji Fujiki^{1,2}, Toshihiro Chikanishi^{1,2}, Waka Hashiba¹, Hiroaki Ito¹, Ichiro Takada¹, Robert G. Roeder³, Hirochika Kitagawa¹, Shigeaki Kato^{1,2}

¹Institute of Molecular and Cellular Biosciences, University of Tokyo, 1-1-1 Yayoi, Bunkyo-ku, Tokyo 113-0032, Japan

²ERATO, Japan Science and Technology Agency, 4-1-8 Honcho, Kawaguchisi, Saitama 332-0012, Japan

³Laboratory of Biochemistry and Molecular Biology, The Rockefeller University, 1230 York Avenue, New York, New York 10021, USA

Abstract

The post-translational modifications of histone tails generate a ‘histone code’ that defines local and global chromatin states¹. The resultant regulation of gene function is thought to govern cell fate, proliferation and differentiation². Reversible histone modifications such as methylation are under mutual controls to organize chromosomal events^{3,4}. Among the histone modifications, methylation of specific lysine and arginine residues seems to be critical for chromatin configuration and control of gene expression⁵. Methylation of histone H3 lysine 4 (H3K4) changes chromatin into a transcriptionally active state⁶. Reversible modification of proteins by β -*N*-acetylglucosamine (*O*-GlcNAc) in response to serum glucose levels regulates diverse cellular processes^{7,8,9}. However, the epigenetic impact of protein GlcNAcylation is unknown. Here we report that nuclear GlcNAcylation of a histone lysine methyltransferase (HKMT), MLL5, by *O*-GlcNAc transferase facilitates retinoic-acid-induced granulopoiesis in human HL60 promyelocytes through methylation of H3K4. MLL5 is biochemically identified in a GlcNAcylation-dependent multi-subunit complex associating with nuclear retinoic acid receptor RAR α (also known as RARA), serving as a mono- and di-methyl transferase to H3K4. GlcNAcylation at Thr440 in the MLL5 SET domain evokes its H3K4 HKMT activity and co-activates RAR α in target gene promoters. Increased nuclear GlcNAcylation by means of *O*-GlcNAc transferase potentiates retinoic-acid-induced HL60 granulopoiesis and restores the retinoic acid response in the retinoic-acid-resistant HL60-R2 cell line. Thus, nuclear MLL5 GlcNAcylation triggers cell lineage determination of HL60 through activation of its HKMT activity.

Reprints and permissions information is available at www.nature.com/reprints.

Correspondence and requests for materials should be addressed to S.K. (uskato@mail.ecc.u-tokyo.ac.jp).

Author Contributions S.K. planned the project and analysed the experiments together with R.F., R.G.R. and H.K. R.F., T.C., W.H., H.I. and I.T. conducted the experiments. The manuscript was written by S.K. and R.F., and all authors commented on it.

Supplementary Information is linked to the online version of the paper at www.nature.com/nature.

Full Methods and any associated references are available in the online version of the paper at www.nature.com/nature.

The currently known RAR co-regulators are unlikely to account for the pluripotent effects of retinoic acid (RA) in cell development¹⁰. Thus, we sought to identify new transcriptional regulators associated with RAR α using biochemical analysis of human HL60 cells¹¹. RAR α -associated regulators were analysed in undifferentiated promyelocyte-like and differentiated granulocyte-like HL60 cells (Fig. 1a). A mass fingerprinting (matrix-assisted laser desorption/ionization–time of flight/mass spectrometry, MALDI-TOF/MS) analysis revealed 43 RAR α interactants (Fig. 1b and Supplementary Table 1). MLL5 was chosen for further study because of its uncharacterized HKMT activity in multisubunit complexes^{12–17}. Like the other MLL members, MLL5 harbours a SET domain, but its sequence bears little homology to those of the other MLL members (Supplementary Fig. 2).

The registered MLL5 gene consists of 27 exons encoding a ~200 kDa protein¹⁴ (Supplementary Fig. 3a), although a much smaller MLL5 isoform (~75kDa) was identified (Fig. 1b). By western blotting with two specific antibodies detecting the amino-terminal (anti-MLL5(N)) and carboxy-terminal (anti-MLL5(C)) regions of the MLL5 protein (Supplementary Fig. 3b), we found that the long form of the MLL5 protein (full-length MLL5, referred to here as MLL5Full) was expressed at much lower levels than the short form (MLL5) in undifferentiated HL60 cells (Fig. 1c) and in human tissues (Supplementary Fig. 4). By mapping a stop site for the short-form messenger RNA in front of exon 15 by rapid amplification of 3'-terminal cDNA ends (3'-RACE) (Supplementary Fig. 5), it was shown that the short isoform is the product of the registered MLL5 gene.

When overexpressed in a transient luciferase assay in undifferentiated HL60 cells, MLL5, but not MLL5Full, co-activated RAR α (Fig. 1d), consistent with knockdown assays using short hairpin RNAs (shRNAs; Supplementary Fig. 6). When the SET domain (362–448 amino acid residues) was deleted (SET) or inactivated (Y358A), RA-induced transactivation by means of RAR α was inhibited (Fig. 1d and Supplementary Fig. 7). In RAR α immunoprecipitates from undifferentiated HL60 cells, significant H3K4 HKMT activity was detected for several histone H3 substrates (H3K4, H3K9, H3K27 and H3K36; Fig. 1e and Supplementary Fig. 8). However, unexpectedly, recombinant MLL5 proteins bacterially prepared were unable to elicit H3K4 HKMT activity *in vitro* (data not shown).

H3K4 HKMT activity was at negligible levels in the HL60-R2 cell line (Fig. 1e), even though MLL5 was expressed at a comparable level (Supplementary Fig. 9). This line is resistant to RA-induced cellular differentiation through an unknown mechanism that does not involve an RAR α gene mutation¹⁸.

An MLL5 complex was isolated from a newly established HL60 stable transformant expressing Flag-tagged MLL5 (Fig. 2a and Supplementary Fig. 10). Corresponding to anti-Flag–MLL5 immuno-complexes (Fig. 2b), Fig. 2c shows two peaks with apparent masses of ~1.5MDa (fractions 18–24, MLL5-L) and ~600kDa (fractions 30–32, MLL5-S). The MLL5-L fraction contained HKMT activity, whereas activity was marginal in the MLL5-S fractions (Fig. 2d).

Two different complexes shared the following common components: serine/threonine kinase 38 (STK38), protein phosphatase 1 catalytic subunits (α , β and γ isoforms; PPP1C α , β and

γ) and β -actin (Fig. 2e, left). Of note, the HKMT-active MLL5-L complex also contained the host cell factor-1 N-terminal subunit (HCF-1N, also known as HCFC1) and *O*-GlcNAc transferase (OGT). Because OGT efficiently binds to wheat germ agglutinin (WGA)¹⁹, we verified the presence of OGT after purification on a WGA column. The eluates then represented the stoichiometric composition of the MLL5-L complex (Fig. 2e, middle), which was further confirmed by western blotting (Fig. 2e, right).

The purified MLL5-L complex, but not MLL5-S (data not shown), methylated nucleosomal H3 in a reconstituted chromatin template (Fig. 2f). We assessed the substrate specificity of the purified MLL5-L complex with several peptides and an artificial H3 N-terminal peptide (1–21), in which Lys 4 was replaced with Ala (K4A). H3K4 was determined to be the MLL5 HKMT target residue (Fig. 2g). Mono-, but not di- nor tri-, methylated H3K4 peptide (1–21) was a good substrate. Methylations were further confirmed by MALDI-TOF/MS (Fig. 2h and Supplementary Fig. 11) and western blotting (Fig. 2i).

On the basis of the inclusion of OGT in the large, active complex, we hypothesized that OGT activates the complex through GlcNAc transfer. GlcNAcylation of the purified complex was confirmed by western blotting with anti-GlcNAc monoclonal antibody (clone number CTD110.6) that specifically recognizes GlcNAcylated Ser/Thr residues (Fig. 3a). Recombinant OGT protein could GlcNAcylate recombinant MLL5 protein *in vitro* (Supplementary Fig. 12) and induce H3K4 HKMT activity (Supplementary Fig. 13).

Addition of the *O*-glycosyl donor UDP-GlcNAc potentiated HKMT activity of the MLL5-L complex, whereas a decoy substrate of OGT, UDP-GalNAc, lacked such an effect (Fig. 3b). The purified MLL5 complex completely lost HKMT activity (Fig. 3b) on conversion into a smaller complex (Supplementary Fig. 14) when the GlcNAcylation moieties of the complex were removed by hexosaminidase (*O*-GlcNAcase) treatment. Thus, GlcNAcylation of OGT and MLL5 appeared necessary to form a large and enzymatically active form of the MLL5 complex.

To define GlcNAcylation site(s) of MLL5, we generated deletion mutants (Supplementary Fig. 15) and individually replaced all 11 Ser and Thr residues in the SET domain with Ala (Fig. 3c). Western blotting identified Thr 440 as a major GlcNAcylation site (Fig. 3c, bottom). This Thr residue is conserved in a putative fly MLL5 homologue (CG9007), but is not present in other MLL family members (Fig. 3c, top). Immunoprecipitates of the MLL5 T440A mutant were enzymatically defective like other catalytically dead SET-domain mutants (Y358A and E441A mutants, Fig. 3d) without overt alteration of protein structure (Supplementary Figs 16 and 17). Potentiation of HKMT activity by UDP-GlcNAc was not seen in similarly prepared immunoprecipitates of the other MLL family members (Supplementary Fig. 18).

MLL5 GlcNAcylation and its HKMT activity depend on the presence of sufficient levels of nuclear UDP-GlcNAc⁷ (Fig. 3e). UDP-GlcNAc is derived from extracellular glucose through the cellular hexosamine biosynthesis pathway (HBP)⁷. Cells were treated with either high-glucose (10–30 mM) media or a GlcNAcase inhibitor (PUGNAc, ~150 μ M) to fully induce nuclear protein GlcNAcylation. Both treatments effectively potentiated RA-

induced differentiation of HL60 into granulocytes (Fig. 4a), but not into other cell types (Supplementary Fig. 19). Suppression of HBP by specific inhibitors (6-diazo-5-oxo-L-norleucine, DON, and azaserine, AZA), which reduced nuclear UDP-GlcNAc level as well as the GlcNAcylation level of MLL5 (Supplementary Fig. 20), attenuated the RA effect (Fig. 4a). This was restored by glucosamine treatment (Supplementary Fig. 21).

Endogenous HKMT activity of MLL5 was much lower in HL60-R2 cells than in HL60 cells (Supplementary Fig. 22). However, treatment with PUGNAc restored responses to RA (Fig. 4b and Supplementary Fig. 23) and RA-induced methylation of histone H3K4 (Fig. 4c and Supplementary Fig. 24). MLL5 was less GlcNAcylated in HL60-R2 cells than in HL60 cells (Fig. 4d), and untreated HL60-R2 cells contained very low levels of intracellular glucose and high *O*-GlcNAcase activity in comparison to HL60 cells (Supplementary Fig. 25), indicating nuclear hypo-GlcNAcylation in HL60-R2 cells.

We monitored RA-induced gene expression of C/EBP ϵ (also known as CEBPE; a major granulopoietic regulator in HL60 cells²⁰) to test the impact of MLL5. C/EBP ϵ gene induction by RA was potentiated by PUGNAc (Fig. 4e, left). Knockdown of MLL5 or OGT by shRNA abrogated RA-induced gene induction. Overexpression of wild-type MLL5, but not the T440A mutant, potentiated the RA effect in HL60 cells, and PUGNAc further enhanced the MLL5 function (Fig. 4e, right). Chromatin immunoprecipitation (ChIP) analysis showed RA-induced recruitment of RAR α and MLL5 complex components to the C/EBP ϵ gene promoter and H3K4 methylation (Supplementary Fig. 26). Similar results were seen in another RAR α target gene, *RARB* isoform 2 (*RARB2*) (refs 10 and 11; Supplementary Fig. 27).

The physiological importance of MLL5 in RA-induced granulopoiesis was tested by MLL5 knockdown using shRNA (Supplementary Fig. 28). In HL60 cells expressing shMLL5-1248 (targeting MLL5 and MLL5Full) or shOGT (based on ZsGreen expression), the capacity of RA to induce granulopoiesis was impaired by 47.5% or 44.9%, respectively (Fig. 4f). It was not inhibited by shRNAs targeting other MLL members (Supplementary Fig. 29).

An enhanced granulopoietic response to RA was detected in HL60 cells overexpressing MLL5 via retroviral vector (Fig. 4g, upper). Under the same experimental conditions, RA-induced granulopoiesis was attenuated in cells expressing either the MLL5 T440A mutant (Fig. 4g, bottom) or the catalytically dead SET domain mutants (Supplementary Fig. 30), presumably by acting as ‘a dominant-negative mutant’ for endogenous GlcNAcylated MLL5.

Here we show that nuclear protein GlcNAcylation facilitates RA-induced differentiation by directly activating MLL5 to di-methylate histone H3K4 (Supplementary Fig. 1). OGT is an indispensable component of the MLL5-L complex required for the GlcNAcylation of MLL5. Recently, two groups reported that, because UDP-GlcNAc levels are controlled through the HBP in response to serum levels of circulating glucose^{21,22}, reversible GlcNAcylation of cytosolic proteins may represent a sensory system for glucose homeostasis. Intracellular transport of OGT from the nucleus to the plasma membrane induced by insulin/phosphoinositide signalling was shown²¹. However, unlike an insulin signal, RA does not induce re-localization of nuclear OGT in HL60 cells (Supplemental Fig. 31). Together with

these previous findings^{8,9,21,22}, it appears that protein GlcNAcylation by OGT is a common post-translational modification of cytosolic and nuclear proteins. Thus, our findings imply that nuclear protein GlcNAcylation is a vital fine-tuning effector in epigenetics.

METHODS SUMMARY

MLL5 and *MLL5Full* cDNAs were isolated from HL60 cells. Both HL60 and HL60-R2 cell lines were maintained in RPMI medium (10% FBS). For HL60 cell granulopoiesis, the cells were treated for 4 days with RA (1 μ M). HL60 cells were infected with the retrovirus under centrifugation at 1,000g for 1h at room temperature (25 °C) in the presence of polybrene (30 μ g ml⁻¹). For assessment of RA-induced differentiation of the infected cells, the cells expressing enhanced green fluorescent protein (eGFP) or ZsGreen, along with *MLL5* constructs or *MLL5*-targeted shRNAs, were analysed by flow cytometry with allophycocyanin (APC)-conjugated anti-CD11b (also known as ITGAM). Biochemical purification using recombinant GST-fused ligand-binding domain of human RAR α (GST-RAR α LBD; 153–462 amino acids) bound to glutathione sepharose was performed as previously described^{23,24}. Nuclear extracts (0.5 g) prepared from RA-treated or -untreated HL60 cells were incubated with 5 μ g of human GST-RAR α LBD with or without RA (1 μ M). The tryptic polypeptides of the individually excised bands were analysed by MALDI-TOF/MS and identified from the peptide mass fingerprints. For purification of the *MLL5* complex, HL60 cells stably expressing Flag-tagged *MLL5* along with the eGFP reporter were concentrated by fluorescence-activated cell sorting (FACS). Using nuclear proteins (0.5 g) derived from the stably transfected cells, the *MLL5*-L complex was isolated by monitoring HKMT activity with the following three purification steps: anti-Flag affinity, gel filtration chromatography with Superose 6 column (GE Healthcare) and WGA lectin agarose. The *in vitro* HKMT and OGT assays were performed as previously reported^{25–27}. Recombinant Flag-*MLL5* and 6 \times His-OGT proteins were prepared by the Bac-to-Bac baculovirus expression system (Invitrogen).

METHODS

Plasmids and retroviruses

Full-length human *MLL5* and *MLL5Full* gene transcripts were amplified from mRNA from HL60 cells. cDNAs of *MLL5*, *MLL5Full* and their deletion mutants, which are fused with Flag tag sequence at their 5' terminals, were subcloned into pMXIG (provided by T. Kitamura) or pcDNA3 (Invitrogen). A series of point mutations in the vectors encoding *MLL5* cDNA was generated with the QuikChange II site-directed mutagenesis kit (Stratagene). shRNA sequences targeting human *MLL5*-742 (5' - GGATCTAGGAAGTCATCAAGA-3'), human *MLL5*-1248 (5' - GGTGAGGCATGAAATTCA AGA-3'), human *MLL5Full*-4476 (5' - GCAACACTCTGTAGCACATGT-3'), human OGT (5' - GCACATAGCAATCTGGCTTCC-3') and *Renilla* Luc (5' - TGCGTTGCTAGTACCAAC-3', as a non-targeting control) were inserted into the pSIREN-RetroQ-ZsGreen vector (Clontech). For retroviral production, the constructed pMXIG and pSIREN-RetroQ-ZsGreen vectors were transfected into PLAT-A cells (provided by T.

Kitamura) with Lipofectamine 2000 reagent (Invitrogen). The culture medium was replaced with fresh DMEM containing 10% FBS 24 h after the transfection, and the cells cultured further for an additional 24 h. The culture supernatant containing the virus was then used for infection.

Cell culture, retroviral infection, differentiation and Giemsa–May–Grunwald staining

HL60 cells were maintained in RPMI medium supplemented with 10% FBS. For retroviral infection, 10^6 cells were suspended in 2 ml of retroviral cocktail (1 ml of the prepared retroviral solution plus 1 ml of RPMI with 10% FBS and $60 \mu\text{gml}^{-1}$ polybrene) and then centrifuged at $1,000g$ for 1 h at room temperature. For granulocytic or monocytic differentiation of HL60 cells, 10^6 cells in the exponential growth phase were exposed to $1 \mu\text{M}$ RA (Sigma) or $1 \mu\text{M}$ VD ($1\alpha,25(\text{OH})_2$ vitamin D3, WAKO). The differentiated cells were cytospun on a glass slide and stained with Giemsa solution (Sigma) and May–Grunwald solution (Sigma) according to the manufacturer's instructions. Flow cytometric analysis and sorting. For flow cytometric evaluation of RA- or VD-induced differentiation, ligand-stimulated cells (10^6) were incubated with $10 \mu\text{gml}^{-1}$ human immunoglobulin G (Sigma) and then immunostained with Alexa Fluor 488- or APC-conjugated anti-human CD11b (BD biosciences), and APC-conjugated anti-human CD 14 (BD biosciences). In the presence of $10 \mu\text{gml}^{-1}$ propidium iodide (Sigma), 2×10^4 cells labelled with the antibodies were analysed with the FACS Caliber system (BD biosciences). A FACS Vantage (BD biosciences) sorter was used to isolate the retroviral-transduced, eGFP-positive cells.

Electroporation and luciferase reporter assay

For the luciferase assays, electroporation was performed by Gene pulser MXcell system (Bio-Rad) at 300 V, 2,000 μF , 1,000 Ω and 10 ms (square-wave pulse). Cells (5×10^6) at the early log phase of growth were electroporated with 25 μg of the indicated plasmids (including 10 μg pGL3 reporters (Promega), 10 μg pRL-null reporters (Promega), 5 μg expression vectors encoding the MLL5 and OGT constructs) in RPMI medium. The electroporated cells were further cultured in the presence or absence of ligand for 48 h. Luciferase activities expressed in the cells were measured with the Dual Luciferase Assay System (Promega).

Immunoprecipitation and immunoblotting

For immunoprecipitation and immunoblotting, whole-cell lysates were prepared with TNE (20mM Tris-HCl, 137 mM NaCl, 10% (v/v) glycerol, 1% (v/v) NP-40, 2mM EDTA, pH 7.9). In the presence or absence of $1 \mu\text{M}$ RA, lysates (1 ml) were immunoprecipitated with anti-RAR α (Santa Cruz) or anti-Flag M2 (Sigma). Immunoblotting was performed with anti-MLL5(N) (Operon Biotechnology), anti-MLL5(C) (MBL), anti-OGT (Sigma), anti-*O*-GlcNAc (CTD110.6, Covance), anti-HCF-1N (Bethyl), anti-STK38 (Abnova), anti-PPP1C α (Upstate), anti-PPP1C β (Chemicon), anti-PPP1C γ (Sigma), anti- β -actin (Santa Cruz) and anti-Flag (Sigma). For the generation of an anti-MLL5(N) antibody, three synthetic peptides, NH₂-Cys1RLGNDKKEMNKS-COOH, NH₂-CEGTTNKMKSPEKQ-COOH and NH₂-Cys1QEPDFIDIEKTP-COOH, individually conjugated to KLH were used as immunogens. To generate MLL5(C) antibody, three KLH-conjugated synthetic peptides, NH₂-Cys+LMEDPDPENPEPTTNEC-COOH, NH₂-CSEKNEKTGKPSDGLSER-COOH

and NH₂-CAQVPPTFQNNYHGSGWH-COOH, were used as immunogens. For immunoblotting of histone methylation, total cell lysates were prepared by sonication in RIPA buffer (50 mM Tris-HCl, 150 mM NaCl, 1% (v/v) NP-40, 0.5% sodium deoxycholate (w/v), 0.1% SDS (w/v), pH 7.9).

ChIP assay

For ChIP analysis, the experimental procedure was basically performed as previously described²⁶. Quantification of the immunoprecipitated DNA was performed by qPCR using Thermal Cycler Dice Real Time System TP800 (TAKARA) and SYBR Premix Ex TaqII (TAKARA). The primers for qPCR were as follows: 5'-ATCCTGGGAGTTGGTGATGTC-3' and 5'-TGCC TCTGAACAGCTCACTT-3' (for RAR β 2 RARE); 5'-AAGTGGGAATGTCCCAT CAGCA-3' and 5'-AGGGCTTCACACCCAGAGCTA-3' (for RAR β 2 distal); 5'-CCACACAGGAGTGGG TGACA-3' and 5'-ATGGAGGCCTCATGCTCACA-3' (for C/EBP ϵ RARE); 5'-TACTGGCAACACAAGCCCAAG-3' and 5'-ACTGCATTCCAGCCCAGGAG-3' (C/EBP ϵ distal).

Biochemical purification using the GST-fused RAR α LBD

Recombinant GST-fused RAR α LBD was expressed in *E. coli*. Nuclear extracts derived from undifferentiated and differentiated HL60 cells were prepared as previously described^{49,50}. Nuclear extracts (0.5 g) were incubated overnight (12 h) with a small amount (<2 μ l) of glutathione sepharose 4B (GE Healthcare), which was saturated with 5 μ g recombinant bait proteins, in the GST purification buffer (50 mM Tris-HCl, 0.1 mM EDTA, 5 mM MgCl₂, 0.5 M KCl, 0.1% (v/v) NP-40, 20% (v/v) glycerol, 2 mM DTT, 1 mM benzamidine, 0.2 mM PMSF, pH 7.9), supplemented with or without 1 μ M RA. The beads were centrifuged along with 40 μ l of additional empty beads and washed with an excess of GST purification buffer. Bound proteins were sequentially eluted three times with 40 μ l of GST purification buffer plus 20 mM glutathione. For identification of the polypeptide, 10 μ l of the 120 μ l eluate was resolved in 4–16% gradient SDS-PAGE. After silver staining with SilverQuest silver staining kit (Invitrogen), visible polypeptides were excised and subjected to tryptic digestion and peptide mass finger print using MALDI-TOF/MS.

Biochemical purification of the Flag-MLL5 complex

HL60 cells stably expressing Flag-MLL5 were established as described in Supplementary Fig. 7 and then cultured in spinner flasks on a 50 l scale. For anti-Flag affinity purification, the prepared nuclear extracts (>0.5 g) were incubated overnight with 50 μ l of anti-Flag M2 resin (Sigma) in buffer D (20 mM Tris-HCl, 0.2 mM EDTA, 5mM MgCl₂, 0.1 M KCl, 0.05% (v/v) NP-40, 10% (v/v) glycerol, 0.5mM DTT, 1 mM benzamidine, 0.2 mM PMSF, pH 7.9). The beads were washed extensively with buffer D and sequentially eluted three times with 50 μ l of buffer D plus 0.3 μ g ml⁻¹ Flag peptide (Sigma). SDS-PAGE and silver-staining analysis was then performed on 2 μ l of the 150 μ l eluates. For gel filtration, 100 μ l of the fractions from the anti-Flag purification was loaded onto a Superose 6 10/300 GL column connected to the AKTA explorer (GE Healthcare) and fractionated with buffer D into 500 μ l fractions. For WGA lectin purification, HKMT active fractions (fractions 18–24) from the gel filtration chromatography were further purified and concentrated with a

glycoprotein isolation kit, WGA (Pierce), according to the manufacturer's instructions. The protein identification was performed as described previously.

Recombinant proteins

Human *MLL5* cDNA fused with Flag, human *OGT* cDNA fused with 6 × His and mouse *HCF1-N* fused with Flag were subcloned into the pFastBac vector (Invitrogen). Recombinant Flag-MLL5, 6 × His-OGT and Flag-HCF-1N were individually expressed in Sf9 cells as described in a previous report²⁷. For purification of Flag-MLL5 and Flag-HCF-1N, whole-cell lysates prepared from the infected cells were combined with TNE350 (TNE supplemented with 350 mM KCl), incubated with anti-Flag M2 resin, washed with TNE, and eluted with TNE supplemented with 0.4 µg ml⁻¹ of Flag peptide. For 6 × His-OGT preparation, 6 × His-OGT was partially purified with HIS-Select Nickel Affinity Gel (Sigma) as previously described²⁷. The eluates were diluted 1:20 with BC0 (20mM HEPES, 0.2mM EDTA, 10% (v/v) glycerol, pH 7.9) and loaded onto a ResourceQ column (BD Healthcare). 6 × His-OGT, fractionated on a linear gradient (0–0.5 M KCl), had a peak at 0.18 M KCl.

In vitro HKMT assay (autoradiographic detection)

For substrate preparation, nucleosomes were reconstituted *in vitro* with purified HeLa histone octamers and plasmid by a salt dilution method. In brief, 5 µg of HeLa histone octamers were incubated with 5.5 µg of plasmid DNA and 2 M NaCl for 15 min at 37 °C. The NaCl concentration of the reaction was serially diluted to 1.5, 1.0, 0.8, 0.7, 0.6, 0.5, 0.4, 0.25 and 0.2 M by adding dilution buffer (50 mM HEPES, 1 mM EDTA, 0.1% NP-40, 5 mM DTT and 0.5 mM PMSF, pH 7.5), with 15 min incubations at 30 °C for each dilution step. The reaction is brought to 0.1 M NaCl by adding a stock buffer (10 mM Tris-HCl, 1 mM EDTA, 0.1% NP-40, 5mM DTT, 0.5 mM PMSF, 20% glycerol). MLL5-L complex was incubated with 0.5 µg of the various substrates (that is, purified HeLa histone H1, purified HeLa histone octamer and the reconstituted nucleosome), in 20 µl reactions of HKMT buffer (20 mM Tris-HCl, 4mM EDTA, 1 mM PMSF, 0.5 mM DTT, pH 7.9) with 0.3 µM (1 µCi) *S*-adenosyl-L-(methyl-³H)methionine (GE Healthcare) for 1 h at 30 °C. The HKMT reaction was stopped by directly adding the SDS-sampling buffer. The reactions were resolved with SDS-PAGE, treated with EN³HANCE (NEN Lifescience), and then subjected to autoradiography with Transcreen-LE intensifying screen (Kodak) and BioMax XAR film (Kodak).

In vitro HKMT assay (mass spectrometric detection)

The following peptides were used: H3 tail (1–21), ARTKQTARKSTGGKAPRKQLA-GG-biocylin (molecular weight of 2,722.2 Da); K4A, ARTAQTARKSTGGKAPRKQLA (2,197.5Da). The purified complexes containing MLL5 and its mutants were incubated with 1 µg of the various histone tail peptides in 50-µl reactions (20 mM Tris-HCl, 4 mM EDTA, 1 mM PMSF, 0.5 mM DTT, pH 7.9) with 0.5 mM *S*-adenosyl-L-methionine (Sigma) for approximately 2 days at 30 °C. An aliquot (2 µl) of the HKMT reaction mixture was diluted 50 times with 0.1% formic acid, and loaded on Poros Tip R2 (PE Biosystems) reversed-phase beads packed into an Eppendorf gel-loading tip. The peptides were deionized by 3 washes with 0.1% acetonitrile and eluted with 30 µl of 30% acetonitrile/0.1% formic acid. A

fraction (3 μ l) of this peptide pool was directly spotted on Prespotted AncorChip (Bruker), dried and subjected to MALDI–TOF/MS analysis using an UltraFlex TOF/TOF instrument (Bruker).

***In vitro* HKMT assay (scintillation detection)**

For peptide substrate analysis, the purified MLL5-L complex and the various immunoprecipitants were incubated with 1 μ g of the various histone tail peptides in 50 μ l reactions of HKMT buffer for 1 h at 30 °C. In the case of the HKMT assay on the immunoprecipitated beads, the reaction was continuously warmed and agitated using BIO Shaker MBR-022 (TAITEC). The reaction was spotted on a P81 paper (Whatman), dried and washed with carbonate buffer (pH9.2). The spotted P81 paper was then soaked with Atomlight fluid (Packard Biosciences) and subjected to liquid scintillation (Beckman).

***In vitro* O-GlcNAcylation assay**

0.5 μ g of 6 \times His-OGT proteins was incubated with 0.5 μ g of Flag-MLL5 and 0.2 mM (0.2 μ Ci) UDP-*N*-acetyl-D-(U-¹⁴C)glucosamine (GE Healthcare) in 25 μ l reactions (50mM Tris-HCl, 12.5mM MgCl₂, 1mM DTT, pH7.5) for 1h at 37 °C. The reactions were resolved with SDS–PAGE, treated with EN³HANCE (NEN Lifescience), and then subjected to autoradiography with Transcreen-LE intensifying screen (Kodak) and BioMax XAR film (Kodak).

Supplementary Material

Refer to Web version on PubMed Central for supplementary material.

Acknowledgements

We thank A. Miyajima and S. Saito for cell lines, P. Chambon, T. Kitamura and S. Suzuki for experimental materials, H. Akaishi for technical support, and M. Yamaki for manuscript preparation. This work was supported in part by priority areas from the Ministry of Education, Culture, Sports, Science and Technology (to H.K. and S.K.).

References

1. Strahl BD & Allis CD The language of covalent histone modifications. *Nature* 403, 41–45 (2000). [PubMed: 10638745]
2. Bernstein BE, Meissner A & Lander ES The mammalian epigenome. *Cell* 128, 669–681 (2007). [PubMed: 17320505]
3. Sarma K & Reinberg D Histone variants meet their match. *Nature Rev. Mol. Cell Biol* 6, 139–149 (2005). [PubMed: 15688000]
4. Li B, Carey M & Workman JL The role of chromatin during transcription. *Cell* 128, 707–719 (2007). [PubMed: 17320508]
5. Zhang Y & Reinberg D Transcription regulation by histone methylation: interplay between different covalent modifications of the core histone tails. *Genes Dev.* 15, 2343–2360 (2001). [PubMed: 11562345]
6. Mikkelsen TS et al. Genome-wide maps of chromatin state in pluripotent and lineage-committed cells. *Nature* 448, 553–560 (2007). [PubMed: 17603471]
7. Hart GW, Housley MP & Slawson C Cycling of *O*-linked β -*N*-acetylglucosamine on nucleocytoplasmic proteins. *Nature* 446, 1017–1022 (2007). [PubMed: 17460662]

8. Jackson SP & Tjian R *O*-glycosylation of eukaryotic transcription factors: implications for mechanisms of transcriptional regulation. *Cell* 55, 125–133 (1988). [PubMed: 3139301]
9. Kelly WG & Hart GW Glycosylation of chromosomal proteins: localization of *O*-linked *N*-acetylglucosamine in *Drosophila* chromatin. *Cell* 57, 243–251 (1989). [PubMed: 2495182]
10. Chambon P A decade of molecular biology of retinoic acid receptors. *FASEBJ.* 10, 940–954 (1996).
11. Collins SJ The role of retinoids and retinoic acid receptors in normal hematopoiesis. *Leukemia* 16, 1896–1905 (2002). [PubMed: 12357341]
12. Nakamura T et al. ALL-1 is a histone methyltransferase that assembles a supercomplex of proteins involved in transcriptional regulation. *Mol. Cell* 10, 1119–1128 (2002). [PubMed: 12453419]
13. Dou Y et al. Physical association and coordinate function of the H3 K4 methyltransferase MLL1 and the H4 K16 acetyltransferase MOF. *Cell* 121, 873–885 (2005). [PubMed: 15960975]
14. Emerling BM et al. *MLL5*, a homolog of *Drosophila trithorax* located within a segment of chromosome band 7q22 implicated in myeloid leukemia. *Oncogene* 21, 4849–4854 (2002). [PubMed: 12101424]
15. Hughes CM et al. Menin associates with a trithorax family histone methyltransferase complex and with the *hoxc8* locus. *Mol. Cell* 13, 587–597 (2004). [PubMed: 14992727]
16. Lee MG et al. Demethylation of H3K27 regulates polycomb recruitment and H2A ubiquitination. *Science* 318, 447–450 (2007). [PubMed: 17761849]
17. Cho YW et al. PTIP associates with MLL3- and MLL4-containing histone H3 lysine 4 methyltransferase complex. *J. Biol. Chem* 282, 20395–20406 (2007). [PubMed: 17500065]
18. Mori J et al. Characterization of two novel retinoic acid-resistant cell lines derived from HL-60 cells following long-term culture with all-trans-retinoic acid. *Jpn. J. Cancer Res.* 90, 660–668 (1999). [PubMed: 10429659]
19. Wysocka J et al. Human Sin3 deacetylase and trithorax-related Set1/Ash2 histone H3-K4 methyltransferase are tethered together selectively by the cell-proliferation factor HCF-1. *Genes Dev.* 17, 896–911 (2003). [PubMed: 12670868]
20. Si J, Mueller L & Collins SJ CaMKII regulates retinoic acid receptor transcriptional activity and the differentiation of myeloid leukemia cells. *J. Clin. Invest* 117, 1412–1421 (2007). [PubMed: 17431504]
21. Yang X et al. Phosphoinositide signalling links *O*-GlcNAc transferase to insulin resistance. *Nature* 451, 964–969 (2008). [PubMed: 18288188]
22. Dentin R et al. Hepatic glucose sensing via the CREB coactivator CRTC2. *Science* 319, 1402–1405 (2008). [PubMed: 18323454]
23. Kitagawa H et al. The chromatin-remodeling complex WINAC targets a nuclear receptor to promoters and is impaired in Williams syndrome. *Cell* 113, 905–917 (2003). [PubMed: 12837248]
24. Ohtake F et al. Dioxin receptor is a ligand-dependent E3 ubiquitin ligase. *Nature* 446, 562–566 (2007). [PubMed: 17392787]
25. Takada I et al. A histone lysine methyltransferase activated by non-canonical Wnt signalling suppresses PPAR- γ transactivation. *Nature Cell Biol.* 9, 1273–1285 (2007). [PubMed: 17952062]
26. Fujiki R et al. Ligand-induced transrepression by VDR through association of WSTF with acetylated histones. *EMBO J.* 24, 3881–3894 (2005). [PubMed: 16252006]
27. Wells L et al. *O*-GlcNAc transferase is in a functional complex with protein phosphatase 1 catalytic subunits. *J. Biol. Chem* 279, 38466–38470 (2004). [PubMed: 15247246]

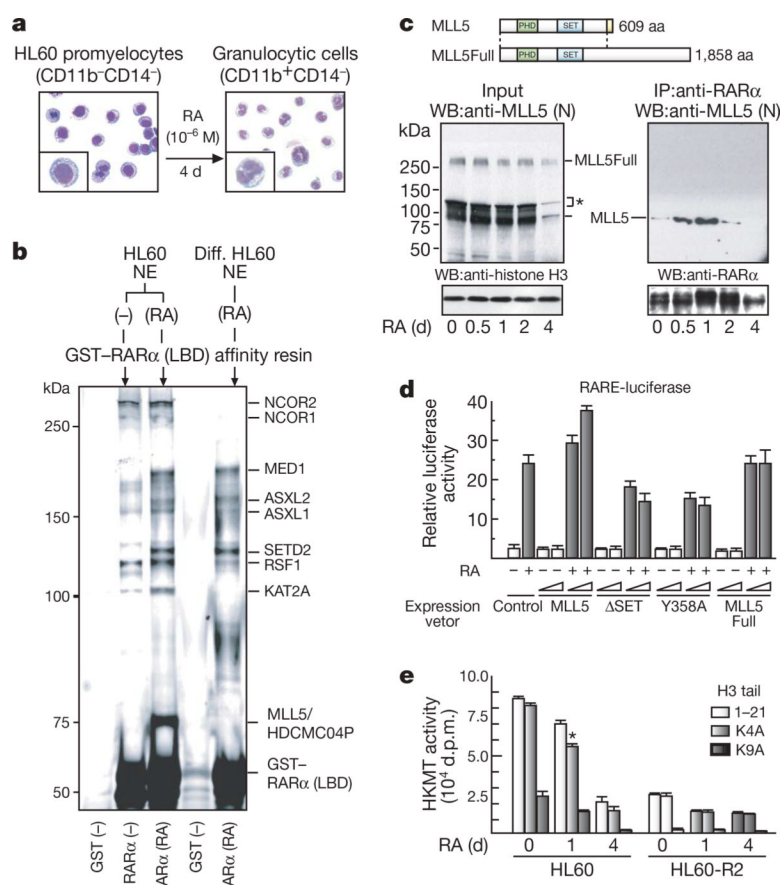


Figure 1 | MLL5 acts as a co-activator of RARα.

a, Giemsa–May–Grunwald staining and cell-surface marker of HL60 cells. **b**, Outline (top) and silver-staining analysis (bottom) of the purification using GST-fused RARα (LBD) as bait. Diff. HL60, differentiated HL60 cells. **c**, Interaction between RARα and MLL5 during RA-induced differentiation. Protein structure of MLL5 (top). The anti-RARα immunoprecipitates (IP) from the RA-treated cells were subjected to western blotting (WB, bottom). The asterisk indicates a nonspecific band. **d**, Luciferase assay of MLL5 function in RAR-mediated transcription. RARE, RA response element. **e**, RARα-associating HKMT activities during RA-induced differentiation. The anti-RARα immunoprecipitants from the differentiating cells were used for *in vitro* HKMT assays with H3 tail peptides (1–21) and the indicated point-mutated peptides. **P* < 0.05 versus the activity for the 1–21 peptide. Error bars, means and s.d. (*n* = 3). d.p.m., disintegrations per minute.

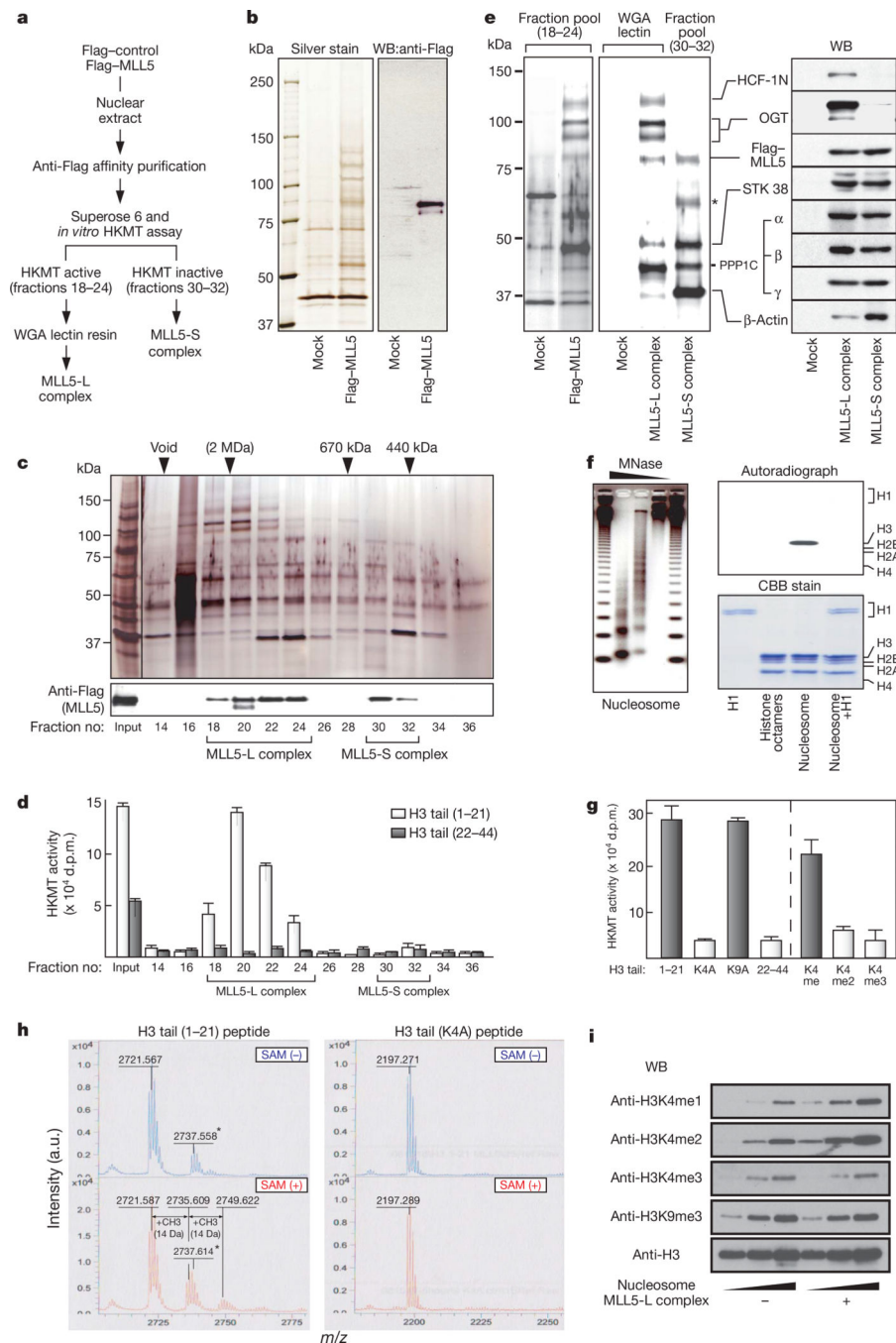


Figure 2 | Purification of the HKMT-active MLL5 complex.

a, Outline of the purification. **b**, **c**, Silver staining and western blot analysis of the anti-Flag affinity purification for the Flag-MLL5 immunocomplex (**b**) and the gel-filtrated fractions (**c**). **d**, HKMT activities of the gel-filtrated fractions using the indicated tail peptides. **e**, Silver staining and western blot (WB) analysis of the MLL5-L and the MLL5-S complexes. The asterisk indicates a nonspecific band. **f**, **g**, Substrate preference of the MLL5-L complex. *In vitro* HKMT assay using the native histone substrates (**f**) and H3 tail peptides (**g**). *In vitro* reconstituted nucleosomes were analysed by micrococcal nuclease assay (MNase assay; **f**).

CBB coomassie brilliant blue. **h, i**, Mass-spectrometric analysis of the H3 tail (1–21 and K4A) peptides (**h**) and western blot analysis of the nucleosomes (**i**) methylated by the MLL5-L complex. The asterisks indicate nonspecific peaks (**h**). Error bars, means and s.d. ($n = 3$). SAM, *S*-adenosyl-L-methionine.

Author Manuscript

Author Manuscript

Author Manuscript

Author Manuscript

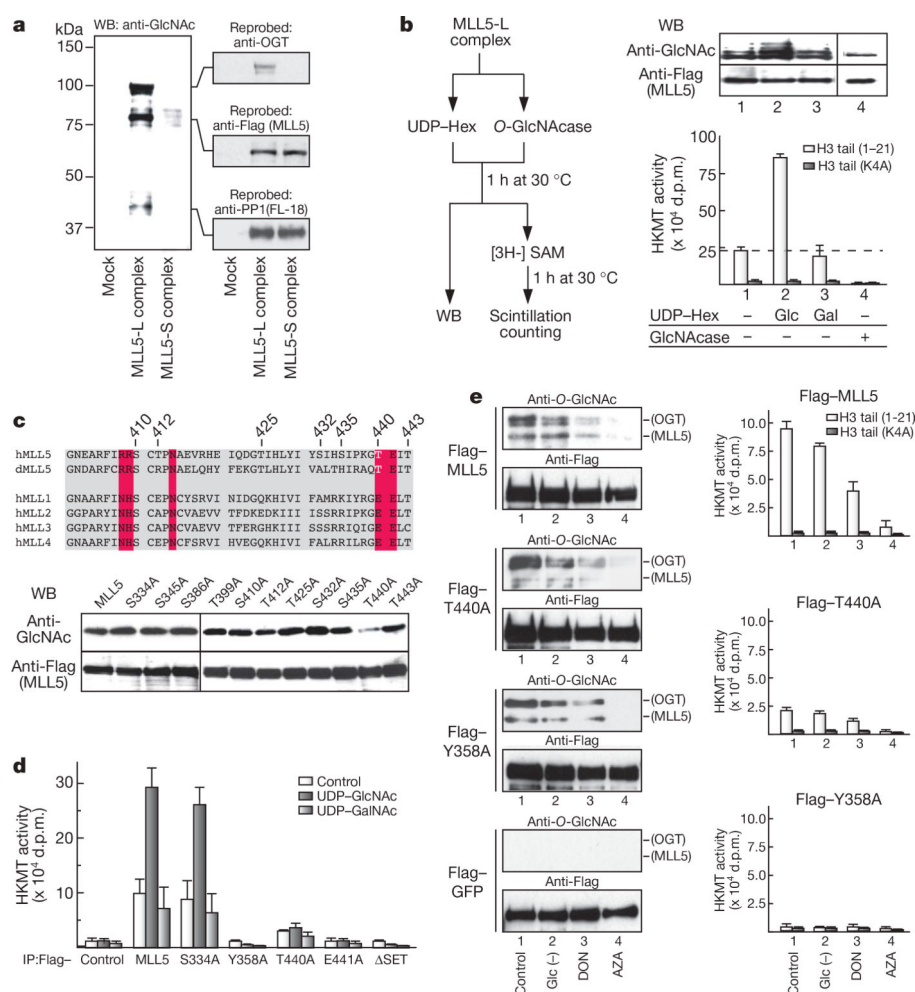


Figure 3 | MLL5 is a GlcNAcylation-dependent HKMT.

a, Western blot (WB) analysis for GlcNAcylation of the MLL5-L and the MLL5-S complexes. The anti-GlcNAc bands were re-probed with the indicated antibodies. **b**, Effect of *in vitro* GlcNAcylation of the MLL5-L complex on its HKMT activity. The experimental procedure is summarized (left). Gal, UDP-GalNAc; Glc, UDP-GlcNAc. **c**, Mapping of GlcNAcylation sites of MLL5. Sequence alignment of MLL-family SET domains (top). The residues required for SAM binding are shaded in red. Western blot analysis for GlcNAcylation of the serial point-mutated MLL5s (indicated Ser/Thr to Ala, bottom). **d**, **e**, GlcNAc-modified (**d**) or -depleted (**e**) MLL5 mutants were subjected to the HKMT assay. GlcNAc levels were analysed by western blot (**e**). Error bars, means and s.d. ($n = 3$).

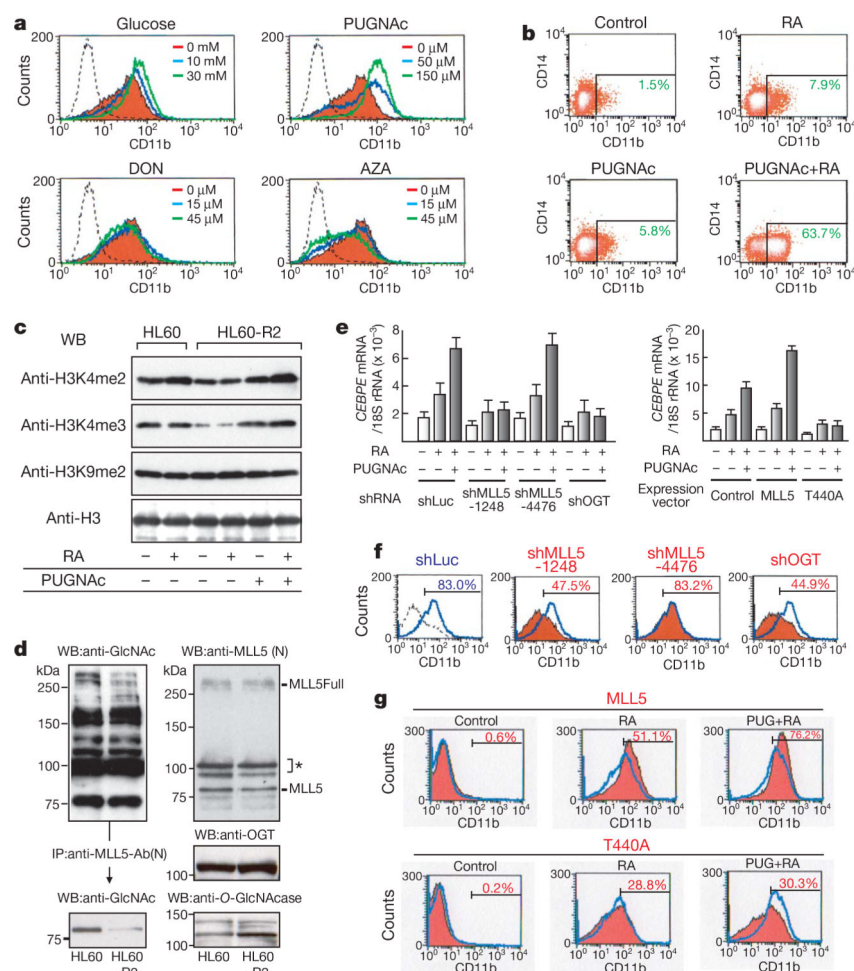


Figure 4 | GlcNAcylation of MLL5 facilitates RA-induced granulopoiesis.

a, b, Effect of cellular GlcNAcylation on RA-induced granulopoiesis. The HL60 cells (**a**) or the HL60-R2 cells (**b**), exposed to the indicated reagents, were analysed by flow cytometry. The dashed line shows RA-untreated control (**a**). **c**, Western blot (WB) analysis for histone H3K4 methylation in the cells treated with RA, PUGNac or both. **d**, Western blot analysis for GlcNAcylation of MLL5 and OGT in HL60 and HL60-R2 cells. **e**, Quantitative polymerase chain reaction (qPCR) analysis of *CEBPE* expression in the cells retrovirally transduced with the indicated shRNAs or expression vectors (using 18S rRNA as internal control). **f, g**, The roles of MLL5 and OGT on RA-induced differentiation. RA-induced differentiation of the HL60 cells, virally expressed with the indicated shRNAs (**f**) or the indicated constructs (**g**), were analysed by flow cytometry. shLuc (**f**) or Flag (**g**) control is overlaid (blue-open). Error bars, means and s.d. ($n = 3$).